

Chapter 1

A Learning Scheme for EMG Based Interfaces: On Task Specificity in Motion Decoding Domain

Minas Liarokapis, Kostas J. Kyriakopoulos, and Panagiotis Artemiadis

Abstract A complete learning scheme for EMG based interfaces is used to discriminate between different reach to grasp movements in 3D space. The proposed scheme is able to decode human kinematics, using the myoelectric activity captured from human upper arm and forearm muscles. Three different task features can be distinguished: subspace to move towards, object to be grasped and task to be executed (with the grasped object). The discrimination between the different reach to grasp movements is accomplished with a random forest classifier. The classification decision triggers task-specific motion decoding models that outperform “general” models, providing better estimation accuracy. The proposed learning scheme takes advantage of both a classifier and a regressor, that cooperate advantageously in order to split the space, confronting with task specificity, the nonlinear relationship between the EMG signals and the motion to be estimated. The proposed scheme can be used for a series of EMG-based interfaces, ranging from EMG based teleoperation of robot arm hand systems to muscle computer interfaces and EMG controlled neuroprosthetic devices.

Keywords ElectroMyoGraphy (EMG) • EMG based interfaces • Learning scheme • Task specificity

M. Liarokapis (✉) • K.J. Kyriakopoulos
National Technical University of Athens, Athina, Greece
e-mail: mliaro@mail.ntua.gr; kkyria@mail.ntua.gr

P. Artemiadis
School for Engineering of Matter, Transport, and Energy, Arizona State University, Tempe,
AZ 85287, USA
e-mail: panagiotis.artemiadis@asu.edu

1.1 Introduction

Electromyography was first used, for the control of advanced prosthetic devices, 30 years ago [1]. Over the last decades, the field of EMG based interfaces has received increased attention, as many applications of mainly surface electromyography (sEMG), have been proposed. Some of those applications are; EMG based teleoperation [2, 3] in remote or dangerous environments, EMG based control of advanced prosthetic limbs [4] that help patients regain lost dexterity, EMG controlled exoskeletons [5] for rehabilitation purposes and muscle computer interfaces as an alternative means for human computer interaction [6] and [7]. Although EMG based interfaces are very promising and may have a vital role in human robot/computer interaction applications for the years to come, some of their disadvantages that have been identified and discussed in many studies in the past are; the high-dimensionality and complexity of the human musculo-skeletal system and the non-linear relationship between the human myoelectric activity and the motion or force to be estimated.

Principal components analysis (PCA) has been used by several studies in the past, for the investigation of human hand kinematic and/or muscle synergies. In [8] optical markers were mounted on 23 different points on the human hand and kinematics were captured during an unconstrained haptic exploration task. PCA was applied in order to conclude to a set of hand postures, representative of most naturalistic postures that appear during object manipulation. The studies conducted by Santello et al. [9] and Todorov et al. [10] identified – capturing the human hand kinematics with datagloves – a limited number of postural synergies “representing” most of the variance, for a wide variety of object grasps. In [11] a similar study was conducted, using a camera-based motion capture system. Regarding muscle synergies, glove measurements combined with EMG activity were acquired in [12], from subjects using the American Sign Language (ASL) manual alphabet, revealing temporal synergies across different muscles, during different hand movements. Muscle synergies ability to formulate a predictive framework, capable to associate muscular co-activation patterns derived from EMGs with new static hand postures, was investigated in [13].

As we have already mentioned one of the main difficulties that researchers face in the field of EMG based interfaces, is the highly nonlinear relationship between the human myoelectric activity and human kinematics, as described in [14]. This difficulty forced the majority of researchers to avoid to decode a continuous representation of human kinematics, choosing to focus on a discrete approach, such as the directional control of a robotic wrist [15] or the control of multifingered robot hands to a series of discrete postures [16, 17] and [18–21]. For doing so, machine learning techniques and more specifically classification methods were used. In [16] and [17] classifiers were used to discriminate based on the human myoelectric activity, between independent human hand’s digit movements or different hand postures. Castellini et al. [22] used forearm surface EMGs for the feed-forward control of a hand prosthesis, discriminating between three different

grip types (power grasp, index precision grip and middle-ring-pinky precision grip), in real-time. Brochier et al. [23] used the myoelectric activity of two adult macaque monkeys, to discriminate muscular co-activation patterns associated with different grasping postures. The latter study was conducted for grasping tasks involving 12 objects of different shapes. Although the discrete EMG based control approach, has been used in many studies and has led to many interesting applications, the use of finite postures may cause severe problems such as the lack of motion smoothness. In fact for most EMG based interfaces (such as the EMG based teleoperation studies), the execution of everyday life tasks that require decoding of complete trajectories, is of paramount importance. Thus, a specification for any proposed methodology, should be to address the issues of continuous and smooth control.

Regarding the continuous EMG based control approach, various techniques have been used to provide estimates of human kinematics based on human myoelectric activity. Some of them are; the Hill-based musculoskeletal model, the state-space model, artificial neural network based models, support vector regression based models and random forests based models. The Hill-based musculoskeletal model [24] is the most commonly used model, for continuous EMG based control of robotic devices, using human motion decoded from EMG signals. Some applications of the Hill-based model can be found in [14] and [25–28]. However the aforementioned Hill model based studies, typically focus on few degrees of freedom (DoFs), because Hill model equations are non-linear and there is a large number of unknown parameters per muscle. State-space models were used by Artemiadis et al. in [2, 29] and [30]. In [29], a state-space model was used to estimate human arm kinematics from the myoelectric activity of muscles of the upper-arm and the forearm, while emphasis was given to the non-stationarity of the EMG signals and the evolution of signal quality over time (i.e., due to muscle fatigue, sweat etc.). In [2] and [30] authors proposed a methodology that “maps” muscular activations to human arm motion, using a state space model and the low dimensional embeddings of the myoelectric activity (input) and kinematics (output). Artificial neural networks (ANN) were used in [31] to estimate the continuous motion of the human fingers, using the myoelectric activity of forearm muscles (only one degree of freedom per finger was decoded), in [32] to control using EMG signals a robot arm with one degree of freedom and in [33] to decode from EMG signals human arm motion, restricting the analyzed movements to single-joint isometric motions.

All the aforementioned studies, addressed the issue of EMG based continuous human motion estimation, but none of them focused on the full human arm-hand system coordination. A Support Vector Machines (SVM) based regressor was used in [3] to decode full arm hand system kinematics. However, only the position and orientation of the human end-effector (wrist) and one DoF for the human grasp, were decoded. Such a choice limits method’s applicability to everyday life scenarios, where independent finger motions are of paramount importance. Finally the latter method requires smooth and slow movements from the user.

In [34, 35] and [36], we proposed a learning scheme that combines a classifier with a regressor to perform task-specific EMG-based human motion estimation for reach to grasp movements. Principal Component Analysis (PCA) was applied to

extract the low dimensional manifolds of the EMG activity and human motion. These low dimensional spaces, were used to train different task-specific models, formulating a regression problem. The scheme was used to discriminate first the task to be executed and trigger then a task-specific EMG based motion decoding model, which achieves better estimation results than “general” models. The estimated output was back projected in the high dimensional space (27 DoFs) to provide an accurate estimate of the full human arm-hand system motion. A similar methodology was recently proposed in [37], where classification techniques were used in order to discriminate between reach to grasp movements towards objects of different sizes and weights. Recently, we extended the learning scheme proposed in [36], in order to discriminate also the “task to be executed”, as well as to perform efficient features selection with random forests [38]. The final scheme discriminates three different task features: position to move towards, object to be grasped and task to be executed (with the object). The scheme consists once again of a classifier combined with a regressor. The classifier uses sEMG to discriminate between different reach to grasp tasks, in the m -dimensional space (where m is the number of EMG channels) of myoelectric activations, while the regressor is used to train models for every possible task. Then based on the classification decision, an appropriate EMG-based task-specific motion decoding model, can be triggered. The regression problem is once again formulated using the low-d spaces of the human EMG signals (input) and the human motion (output). It must be noted that for these last five studies the classification accuracy constantly increases – as the reach to grasp movement evolves – providing always an early decision (at the beginning of reach to grasp movement) of the task to be executed.

In this chapter we formulate a complete learning scheme for EMG based interfaces, that takes advantage of a classifier which is combined with a regressor. The classifier and the regressor cooperate advantageously in order to split the task space and provide better estimation accuracy, with task specific models. The whole scheme is based on the random forests methodology for classification and regression. EMG signals are used to discriminate different reach to grasp movements in 3D space. Task specificity is introduced in three different levels, suggesting that the myoelectric activity differentiates; between reach to grasp movements towards different subspaces, between reach to grasp movements towards different objects, as well as between reach to grasp movements towards a specific object placed at a specific position, but with the intention to perform different tasks while the object is grasped. The classifier uses the human myoelectric activity, to discriminate between those different reach to grasp movements in the m -dimensional space of the EMG signals (m is the number of channels). The regressor is first used to train task-specific models for all possible tasks, so as for a task-specific model to be triggered, based on the classification decision. Classification decision is taken at a frequency of 1 kHz, enabling our scheme to identify the task in real time. The proposed scheme can provide continuous estimates of the full human arm hand system kinematics (27 DoFs modeled, 7 for the human arm and 20 for the human hand). Those estimates can be used by a series of EMG based interfaces.

The rest of the chapter is organized as follows: Sect. 1.2 analyzes the apparatus and the experiments conducted, Sect. 1.3 focuses on the different methods used to formulate the proposed EMG-based learning scheme, results for EMG based classification and task specific EMG based motion estimation are presented in Sect. 1.4, while Sect. 1.5 concludes the chapter.

1.2 Apparatus and Experiments

1.2.1 *Experimental Protocol*

Two different types of experiments were conducted for the formulation of the proposed learning scheme. All experiments were performed by five (4 male, 1 female) healthy subjects 21, 24, 27, 28 and 40 years old. The subjects gave informed consent of the experimental procedure and the experiments were approved by the Institutional Review Board of the National Technical University of Athens. Experiments were performed by all subjects, using their dominant hand (right hand for all subjects involved).

During experiments the subjects were instructed to perform different reach to grasp movements in 3D space, to reach and grasp different objects placed at different positions, in order to execute different tasks with the grasped objects. The object positions were marked on different shelves of a bookcase, as depicted in Fig. 1.1.

The first type of experiments, involved reach to grasp movements towards different positions (five different positions depicted in Fig. 1.1) and different objects (a mug, a rectangular shaped object and a marker) and was used for EMG-based “subspace discrimination” and “object discrimination”. The second type of experiments, involved reach to grasp movements towards specific positions and objects, in order to execute two different tasks (two classes), with the same object. A tall glass, a wine glass, a mug and a mug plate were used for the second type of task discrimination experiments. The first experiments were used for the initial formulation of the learning framework proposed in [34] and were once again used in [38] together with the second type of experiments, to discriminate between different tasks and compute feature variables importance for different positions, objects and tasks.

The tasks executed for the second type of experiments appear in Fig. 1.2. During the experiments, each subject conducted several trials, for each position, object and task combination. In order to ensure data quality and avoid fatigue, adequate resting time of 1 min, was used between consecutive trials.

1.2.2 *Motion Data Acquisition*

In order to capture efficiently human kinematics – using appropriate motion capture systems – the kinematic models of the human arm and the human hand must

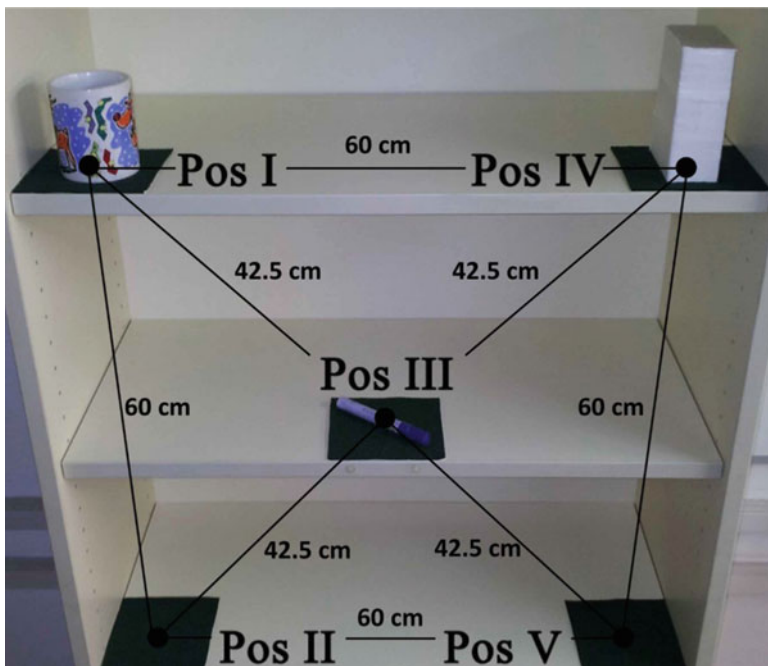


Fig. 1.1 A bookcase containing three different objects (a marker, a rectangular-shaped object and a mug), placed at five different positions, at three different shelves, is depicted. A superimposed diagram presents the distances between the different object positions. These five positions were used for both types of experiments



Fig. 1.2 Tasks executed for the second type of experiments. The tall glass tasks were: task 1, side grasp (to drink from it) and task 2, front grasp (to transpose it). The wine glass tasks were: task 1, side grasp (to drink from it) and task 2, stem grasp (to drink from it). The mug tasks were: task 1, handle grasp (to drink from it) and task 2, top grasp (to transpose it). Finally the mug plate tasks were: task 1, side grasp (to lift and hold it) and task 2, top grasp (to transpose it)

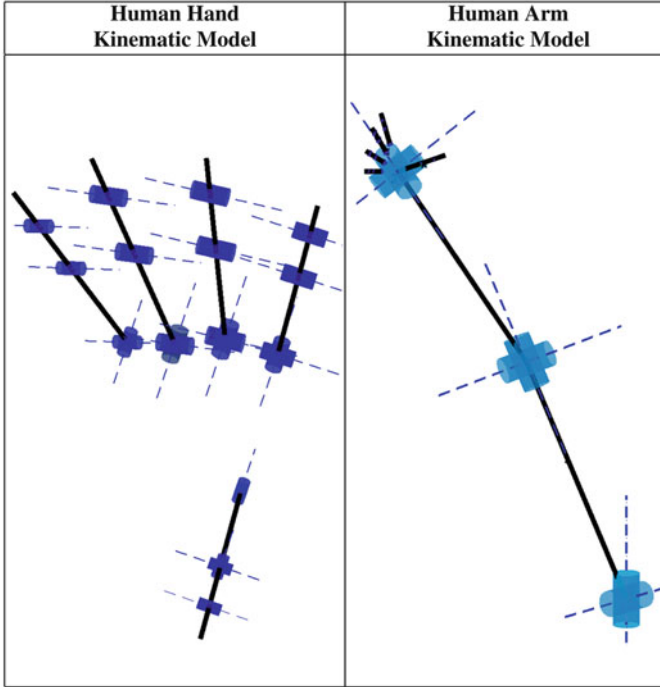


Fig. 1.3 Kinematic models depicting the degrees of freedom (DoFs) of the human arm and hand

be described. The kinematic model of the human arm, that we use in this study, consists of three rotational degrees of freedom (DoFs) to model shoulder joint, one rotational DoF for elbow joint, one rotational DoF for pronation-supination and two rotational DoFs for wrist flexion/extension and abduction/adduction. The kinematic model of the human hand consists of 20 rotational DoFs, 4 for each one of the 5 fingers. Regarding fingers we used for the four kinematically identical fingers (index, middle, ring and pinky) three rotational DoFs to model flexion-extension of the different joints and one rotational DoF for abduction-adduction. Human thumb is modeled, using two rotational DoFs for flexion-extension, one rotational DoF for abduction-adduction and one rotational DoF to describe palm's mobility that allows thumb to oppose to other fingers. The kinematic models of the human arm and hand are presented in Fig. 1.3.

In order to capture the human arm hand system motion in 3D space, extracting the corresponding joint angles (27 modeled DoFs), we used a dataglove for the human hand and a magnetic position tracking system for the human arm. The Isotrak II[®] (Polhemus Inc.) magnetic motion capture system used, is equipped with two position tracking sensors and a reference system. The two sensors of Isotrak II, were placed on the elbow and the wrist respectively, while the reference system was placed on the user's shoulder. Having captured the positions of the human shoulder, elbow and wrist, the inverse kinematics of the human arm can

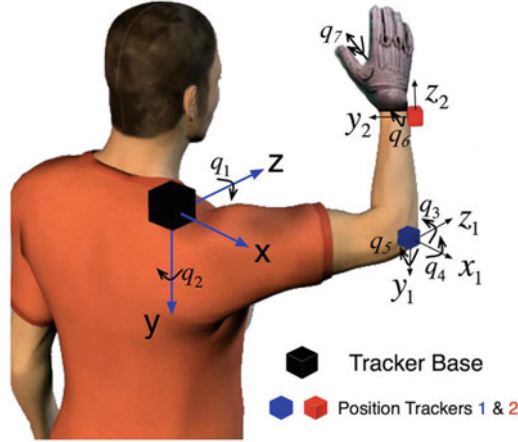


Fig. 1.4 Two position tracking sensors of Isotrak II are used to capture user's shoulder, elbow and wrist position in 3D space, while a dataglove is used to capture the wrist and fingers joint angles. The position tracker reference system is placed on the shoulder. The human arm joint values can be computed through the human arm's inverse kinematics. q_1 and q_2 jointly correspond to shoulder flexion-extension and adduction-abduction, q_3 to shoulder internal-external rotation, q_4 to elbow flexion-extension, q_5 to pronation-supination and q_6 and q_7 jointly correspond to wrist flexion-extension and adduction-abduction

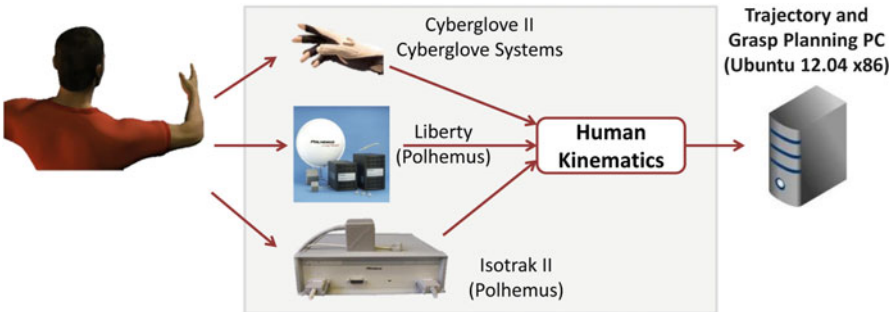


Fig. 1.5 Different motion capture systems, used to capture human arm hand system motion, are depicted

be computed, following the directions provided in [39]. Alternatively for human robot interaction applications, a human to robot motion mapping procedure like the one proposed in [40], can be used. Regarding the human hand, the Cyberglove II[®] (Cyberglove Systems), is used to measure the 2 DoFs of the wrist (flexion-extension and abduction-adduction) and the 20 DoFs of the human fingers. The experimental setup that was used to track human arm hand system kinematics, is depicted in Fig. 1.4 and the different motion capture systems are depicted in Fig. 1.5.

1.2.3 Electrode Positioning and EMG Data Acquisition

In total, we recorded the myoelectric activity of 16 muscles, of the upper arm (8 muscles) and the forearm (8 flexor and extensor muscles). More specifically the chosen muscles are: flexor pollicis longus, flexor digitorum superficialis, flexor carpi ulnaris, flexor carpi radialis, extensor pollicis longus, extensor indicis, extensor carpi ulnaris, extensor carpi radialis, deltoid anterior, deltoid posterior, deltoid middle, trapezius, teres major, brachioradialis, biceps brachii and triceps brachii. The selection of the muscles and the placement of the surface electromyography electrodes, was based on the related literature [16, 41]. In order to achieve easy, portable and fast to use training schemes several researchers have chosen to place the EMG electrodes, in specific regions but in random (not precise) positions [3]. We believe that the next generation of epidermal electronics [42] will make the electrode positioning faster and easier, thus we choose to take advantage of the higher signal to noise ratio, that accurate electrode positioning offers.

EMG signals were acquired and conditioned using an EMG system (Bagnoli-16[®], Delsys Inc.), equipped with single differential surface EMG electrodes (DE-2.1[®], Delsys Inc.). A signal acquisition board (NI-DAQ 6036E[®], National Instruments), was used for signal digitization and data acquisition.

1.2.4 EMG and Motion Data Processing

Regarding data processing, EMG signals were band-pass filtered (20–450 Hz), sampled at 1 kHz, full-wave rectified and low-pass filtered (Butterworth, fourth order, 8 Hz), while for the position measurements, which were provided by the position tracking system at the frequency of 30 Hz, an antialiasing finite-impulse-response filter (low pass, order: 24, cutoff frequency: 100 Hz), was used to resample them at a frequency of 1 kHz (same as the sampling frequency of the EMG signals).

1.2.5 Muscular Co-activation Patterns Extraction

After data collection, all EMG recordings, were pre-processed and epochs of data were created. Those epochs included the different reach-to-grasp movements captured during the experiments. Then, all data were resampled at 100 Hz, where each sample at the new frequency (100 Hz) was calculated as the mean value of ten (10) samples of the original frequency (1 kHz). Based on the profiles of the rectified EMG signals at the new frequency, the onset of muscular activations was defined comparing the amplitude of each muscle's myoelectric activation to its relaxed state. Finally, epochs including only muscular activations captured during the actual

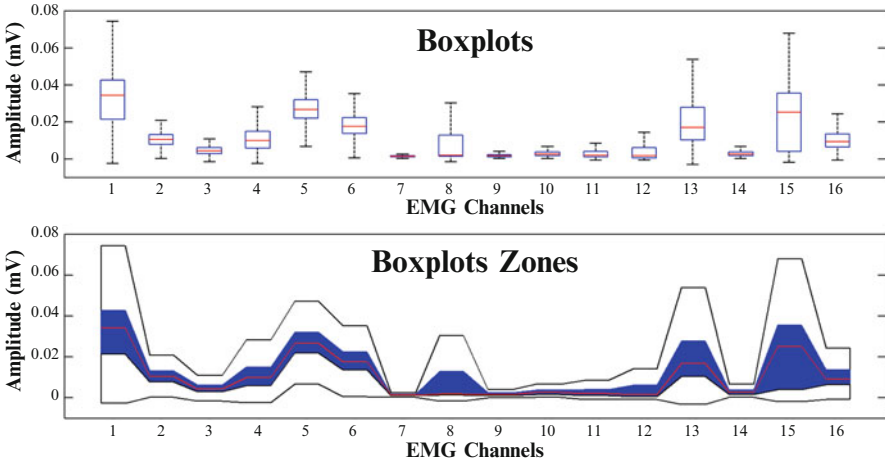


Fig. 1.6 Comparison of a Boxplot and a “Boxplot Zone” visualization of muscular co-activation patterns across sixteen (16) muscles of the upper arm and the forearm for one subject (Subject 1), performing reach to grasp movements towards a mug placed at position I

tasks were created, and were used to formulate synergistic profiles, using a novel statistical representation technique, that we introduced and which we call “Boxplot Zones”.

A boxplot (alt. box-and-whisker plot) is a method to graphically depict groups of numerical data, through the following five-number summaries: smallest observation (sample minimum), lower quartile (Q1), median (Q2), upper quartile (Q3), and largest observation (sample maximum). Boxplot zones were first defined in [34] to visualize muscular co-activation patterns and are an equivalent of boxplots, while more visually informative representation, suitable for the representation of synergistic profiles. Boxplot zones consist of three different layers. The first layer includes the median line, connecting the medians of all boxplots. The second layer includes the box zone (blue zone), connecting the boxes that contain all the values between the lower and the upper quartile, while the third layer includes the whisker zone (white zone), connecting the whiskers that mark the largest and the smallest observation. A direct comparison of a boxplot and a boxplot zone visualization, can be found in Fig. 1.6.

In Fig. 1.7 we present a “boxplot zones” based visualization of muscular co-activation patterns of sixteen (16) muscles (of the upper arm and the forearm), for one subject (Subject 1) executing reach to grasp movements, towards five (5) different positions in 3D space, to grasp three (3) different objects. The muscular co-activation patterns presented in Fig. 1.7 in terms of synergistic profiles formulated with boxplot zones, depict a significant differentiation between the different reach-to-grasp movements, although the same joints of the arm hand system (human upper arm joints and human hand finger joints) are involved, but for a different task. More precisely, if we examine the synergistic profiles (muscular co-activation patterns)

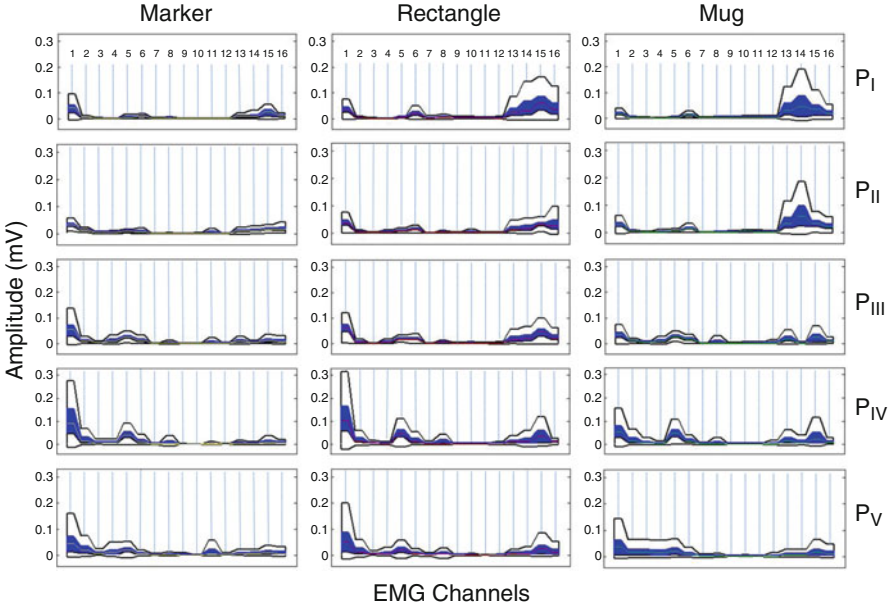


Fig. 1.7 “Boxplot Zones” visualization of muscular co-activation patterns of sixteen (16) muscles (of the upper arm and the forearm), for one subject (Subject 1) performing reach to grasp movements towards, five different positions (P_I , P_{II} , P_{III} , P_{IV} and P_V) in 3D space, to grasp three different objects (a marker, a rectangle and a mug). The sixteen (16) muscles are reported in the following order (1–16): deltoid anterior, deltoid middle, deltoid posterior, teres major, trapezius, biceps brachii, brachioradialis, triceps brachii, flexor pollicis longus, flexor digitorum superficialis, flexor carpi ulnaris, flexor carpi radialis, extensor pollicis longus, extensor indicis, extensor carpi ulnaris and extensor carpi radialis

across different subspaces (different positions), we notice that the activity of the muscles of the upper-arm (EMG channels 1–8) reflects most of the differentiation. In contrast, if we examine the muscular co-activation patterns across different objects, placed in the same subspace (a specific position), the activity of the muscles of the forearm (EMG channels 9–16) reflects most of the differentiation.

In Fig. 1.8 we present a “boxplot-zones” based visualization of muscular co-activation patterns differentiation, for 16 muscles of the human upper-arm and forearm, for 3 different subjects performing different reach to grasp movements, towards five (5) different positions in 3D space, to grasp a specific object (rectangular-shaped object).

As we have already noted there is a significant differentiation between muscular co-activation patterns associated with different reach to grasp movements. Statistical significance of muscular co-activation patterns differentiation, can be assessed using appropriate statistical tests. More precisely the Lilliefors test (adaptation of the Kolmogorov-Smirnov test) was used to test the null hypothesis that the EMG data – containing the myoelectric activations – come from a normal distribution. The test rejects the null hypothesis at the 5% significance level ($p = 0.05$), so the

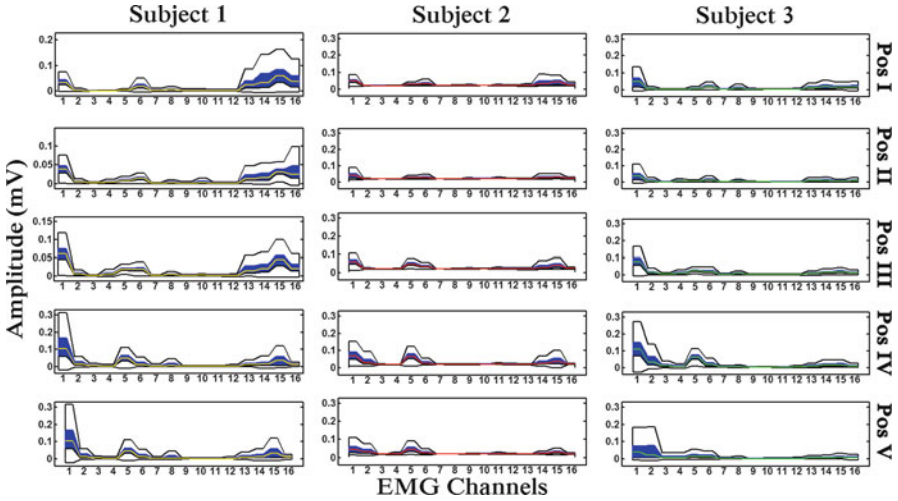


Fig. 1.8 “Boxplot Zones” visualization of different muscular co-activation patterns of sixteen (16) muscles of the upper arm and the forearm, for three (3) different subjects performing reach to grasp movements towards, the aforementioned five (5) positions in 3D space, to grasp a specific object (a rectangle)

data are not normally distributed. Thus, we use non parametric tests such as, the Kruskal-Wallis and the Wilcoxon rank sum test, in order to assess the significance of muscular co-activation patterns differentiation, for different strategies.

The Kruskal-Wallis compares the medians of the myoelectric activity of the selected muscles, for different muscular co-activation patterns, and returns the p value for the null hypothesis that all samples are drawn, from the same population (or from different populations with the same distribution). The Wilcoxon rank sum test, performs a two-sided rank sum test of the null hypothesis that data of myoelectric activations with different muscular co-activation patterns, are independent samples from identical continuous distributions, with equal medians.

More details regarding the statistical procedures used, the reader can find in [43]. All tests were performed to check the differentiation of muscular co-activation patterns for the following three cases:

- For the same reach to grasp movement, between different subjects.
- For reach to grasp movements towards five different positions in 3D space.
- For reach to grasp movements towards three different objects, placed at a specific position in 3D space.

For all sets, confidence levels were set at 95 %. All tests null hypotheses for all three cases were rejected, proving that muscular co-activation patterns differentiate, between different subjects and between different tasks. In Fig. 1.9, we present the means and the confidence intervals of EMG activity across eight muscles of the upper arm and eight muscles of the forearm, for a subject performing reach to grasp movements, towards three (3) different objects. In Fig. 1.10, we present the means

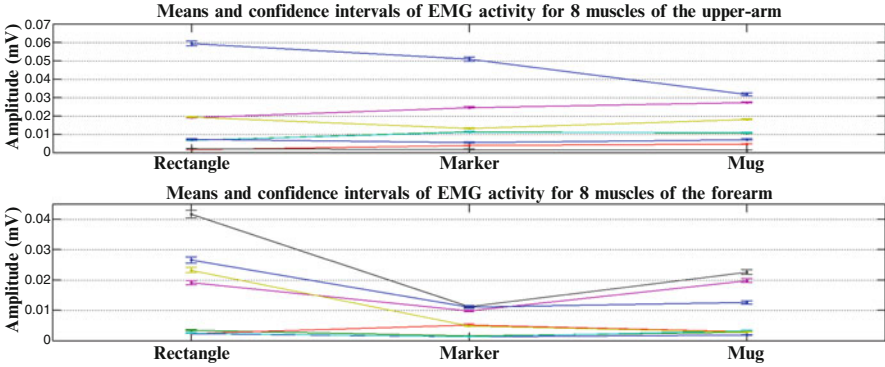


Fig. 1.9 Means and confidence intervals of EMG activity across eight (8) muscles of the upper arm and eight (8) flexor and extensor muscles of the forearm, for one subject (Subject 1) performing reach to grasp movements, towards three (3) different objects, placed at a specific position (Pos 3) in 3D space

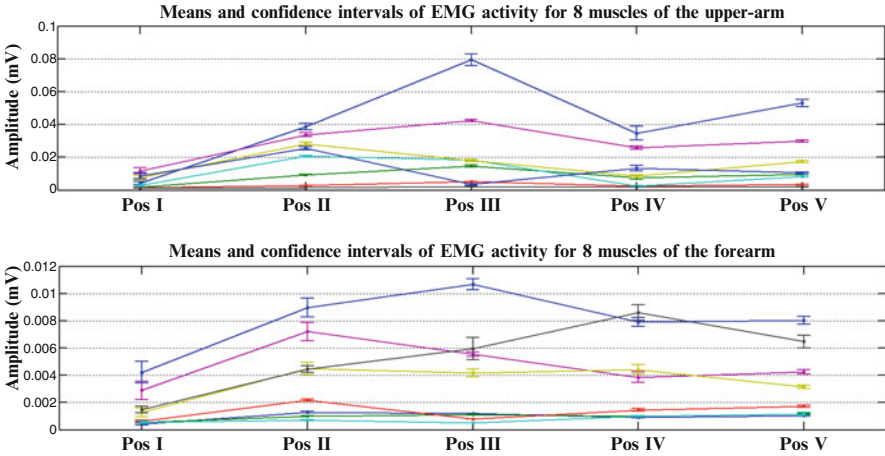


Fig. 1.10 Means and confidence intervals of EMG activity across eight (8) muscles of the upper arm and eight (8) flexor and extensor muscles of the forearm, for one subject (Subject 1) performing reach to grasp movements, towards a marker, placed at five (5) different positions in 3D space

and the confidence intervals of EMG activity across eight muscles of the upper arm and eight muscles of the forearm for a subject performing reach to grasp movements, towards a marker, placed at five (5) different positions in 3D space.

Therefore, we conclude that the muscular co-activation patterns vary significantly not only between different subjects, but also between different reach-to-grasp movements of the same subject (towards different subspaces or different objects placed at specific position), and therefore should be considered and analyzed as subject-specific and task-specific characteristics.

1.3 Methods

In this section we present some typical specifications for EMG based interfaces and we describe the problem formulation and the methods used for discrimination of different muscular co-activation patterns, associated with different reach to grasp movements (classification) and EMG based motion estimation (regression).

1.3.1 *Classification and Regression Modules*

Some specifications that every EMG-based learning scheme should have, are:

- To be able to “decide” on user’s intention (classification part).
- To decode a continuous representation of human motion (regression part).
- To allow its application at a robot control scheme, in real time.
- To be easy and fast to be trained for different users (as musculoskeletal characteristics may vary significantly across subjects).
- To be able to handle multidimensional spaces and large databases of myoelectric and motion data.

In this chapter we present an EMG-based learning scheme, using the Random Forests (RF) technique – which meets the aforementioned specifications – for both classification and regression. Thus, the classifier and the regressor cooperate advantageously, in order to split the task space and confront the non-linear relationship between the EMG signals the motion to be estimated, with task specific models that provide better estimation accuracy than the “general” models (built for all tasks).

In Fig. 1.11 we present a block diagram of a typical random forests based classification procedure. Random forests are used for a multiclass classification problem, where we need to discriminate between reach to grasp movements, towards different positions, different objects (to be grasped) and different tasks (to be executed with the object) in 3D space, using human myoelectric activity (EMG).

In Fig. 1.12 we present the block diagram for a typical random forests based regression procedure. The task specific models trained are used to estimate for new EMG data (not previously seen during training) “new” human arm hand system kinematics.

A complete block diagram of the EMG-based learning scheme proposed, is depicted in Fig. 1.13. Two main modules appear, the classification module and the task specific model selection module. Classification module provides decision for subspace to move towards, object to be grasped and task to be executed (with the object). Task specific model selection module, examines classification decisions and triggers a subspace, object and task specific motion decoding model.

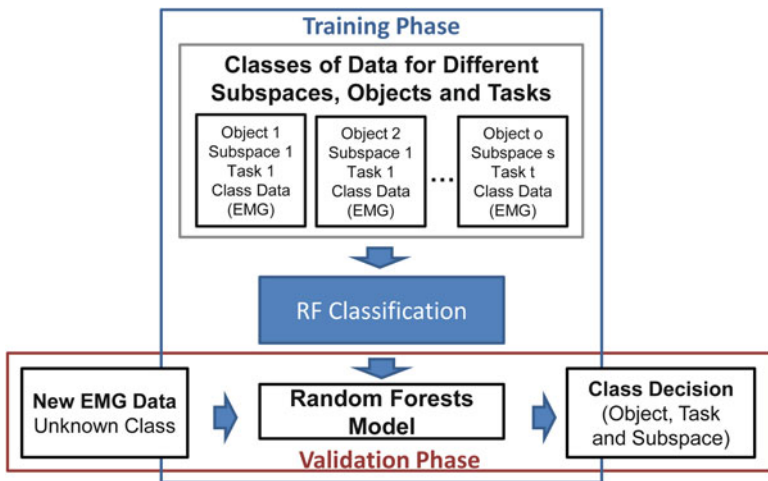


Fig. 1.11 Block diagram of the classification procedure

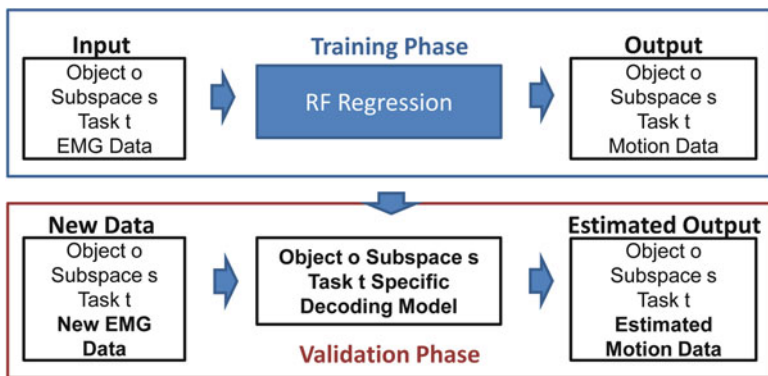


Fig. 1.12 Block diagram of the regression procedure

1.3.2 Multiclass Classification in the m -Dimensional Space of Myoelectric Activations (m -Number of EMG Channels)

As we have already noted, synergistic profiles depicted in terms of “boxplot zones” in Fig. 1.7 denote that there is a significant differentiation of muscular co-activation patterns for reach to grasp movements towards different positions and different objects placed at the same position. In order to be able to take advantage of this differentiation, we choose to discriminate the different reach to grasp movements

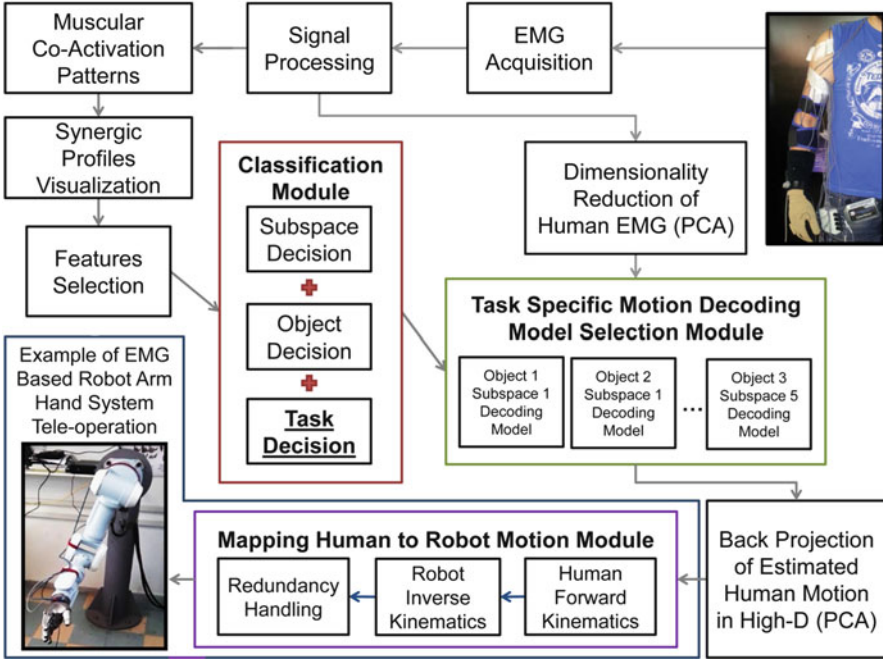


Fig. 1.13 A block diagram of the proposed EMG-based learning scheme is presented. Two main modules, formulate the “backbone” of the learning scheme, the classification module and the task specific model selection module. Classification module (based on the classifier) provides decision for subspace to move towards, object to be grasped and task to be executed with the object. Task specific model selection module (based on the regressor) examines classification decisions and triggers a subspace, object and task specific motion decoding model (from all possible models trained). The task specific motion decoding model efficiently estimates the full human arm hand system motion (27 joint values), using human myoelectric activity (EMG signals). Finally an EMG-based interface can take advantage of the proposed scheme and the estimated human motion. For example a human to robot motion mapping procedure may take as input the estimated human arm hand system motion, to generate equivalent robot motion, as described in [40]. A possible application of the proposed learning scheme, is the EMG-based teleoperation of a robot arm hand system

in the m -dimensional space of the myoelectric activations (where m is the number of EMG channels), using the EMG signals to “decide” on the task to be performed (human intention decoding).

In Fig. 1.14 we present a typical classification problem of discriminating based on the myoelectric activity of 16 muscles of the human arm hand system, two different strategies for reaching and grasping a specific object placed in two different positions. Reaching, grasping and return phases are depicted. The top subplot presents the distance between the two classes in the 16-dimensional space (16 EMG channels are used). Such a distance, give us a measure of classes separability (i.e., how easily these classes can be discriminated). The bottom subplot, presents the evolution of classification decision over time. The accumulation of misclassified

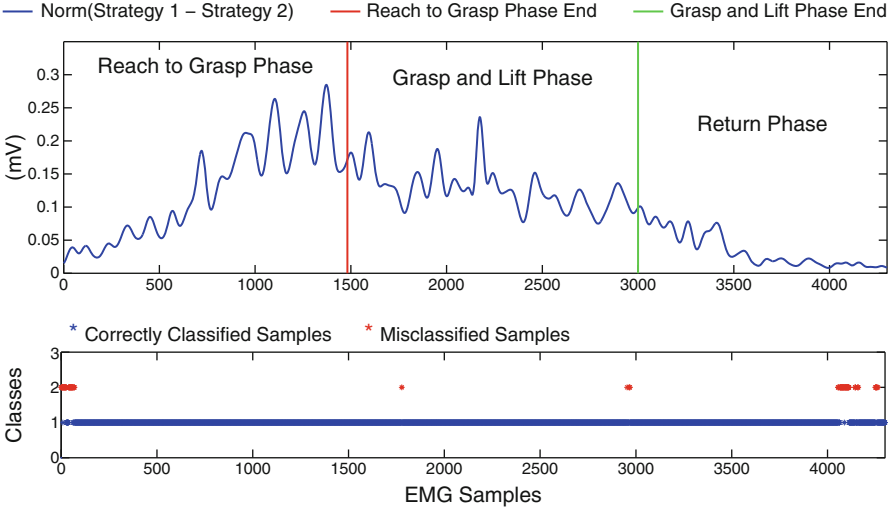


Fig. 1.14 Comparison of two reach to grasp movements towards a marker placed at position I (Strategy I) and a marker placed at position II (Strategy II). First subplot presents the distance of the two strategies in the m -dimensional space (where $m = 16$ the number of the EMG channels). The second subplot focuses on the evolution of classification decision per sample, over time

samples is reasonable for those time periods, when the distance between the two classes is small (i.e. begin and end of experiments, when human end-effector (wrist), is close to its starting position).

In Fig. 1.15 we present the classification problem of discriminating two different reach to grasp movements, towards a specific object placed at a specific position, but in order to execute two different tasks (with the object). Once again, top subplot presents the distance between the two classes in the 15-dimensional space (15 EMG channels are used), as well as the reaching, grasping and return phases. Bottom subplot presents once again the evolution of the classification decision and there is a similar with Fig. 1.14, accumulation of misclassified samples for the time periods, that the distance between the two tasks is small (i.e. begin and end of the experiment).

1.3.2.1 Random Forests Classifier

The Random Forests technique proposed by Tin Kam Ho of Bell Labs [44] and Leo Breiman [45], can be used for classification creating an ensemble classifier that consists of many decision trees. The Random Forests classifier's output, is the class that is the mode of the individual trees class's output. Thus, the classifier consists of a collection of tree structured classifiers $\{h(\mathbf{x}, \Theta_N), N = 1, \dots\}$ where $\{\Theta_N\}$ are independent identically distributed random vectors. Each decision tree of the random forest, casts a vote for the most popular class at input \mathbf{x} .

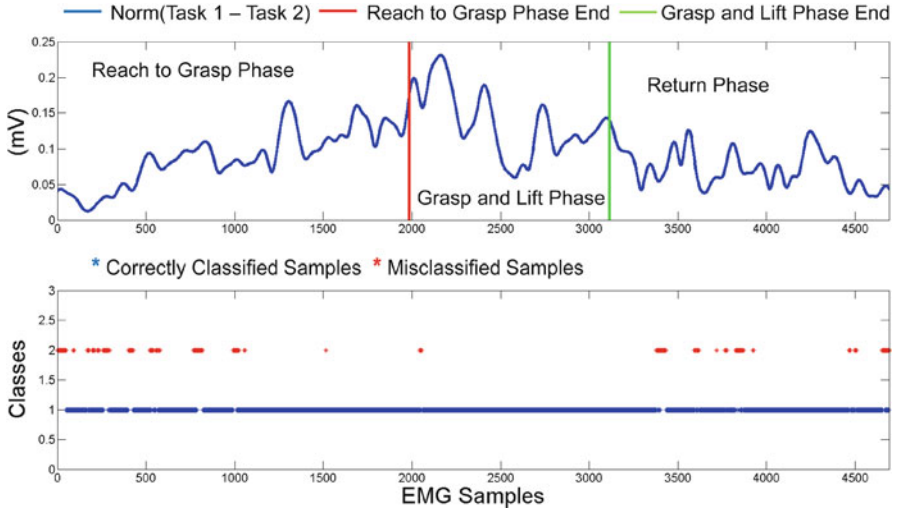


Fig. 1.15 Comparison of two reach to grasp movements, towards Position I to grasp a tall glass with two different grasps (side grasp and front grasp), to execute two different tasks. First subplot presents the distance of the two tasks in the m -dimensional space (where $m = 15$ the number of the EMG channels). The second subplot focuses on the evolution of classification decision per sample, over time

The classification procedure for N trees grown is presented in Fig. 1.16. Some advantages of the random forests technique for classification are:

- Runs efficiently and fast on large databases.
- Provides high accuracy.
- Does not overfit.
- Provides feature variables importance.
- Can handle thousands of input variables without variable deletion.
- Can handle multiclass classification problems.
- Can be used efficiently in multidimensional spaces.

1.4 Features Selection with Random Forests

In the aforementioned classification examples we used the random forests technique to discriminate, between different reach to grasp movements in the m -dimensional space of the myoelectric activations, using multiple EMG channels (m is 15 or 16). Its quite typical for EMG based interfaces, a limited number of EMG channels to be available (e.g., due to cost or complexity limitations), or EMG electrodes positioning to be not precise (some EMG channels may be more noisy). Thus, a fundamental question is: “Is it possible to select which EMG channels are the

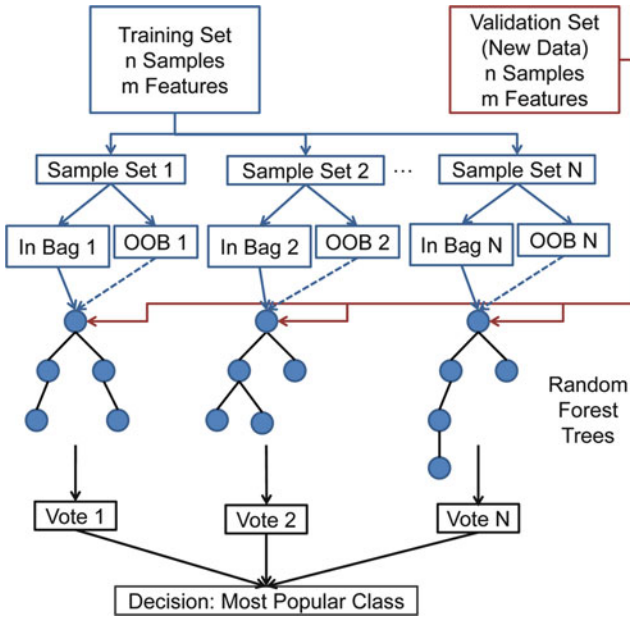


Fig. 1.16 Random forests based classification procedure for N trees grown. OOB stands for out-of-bag samples

most important? How this features selection can be accomplished?”. With Random Forests we can perform efficient features selection, using their ability to compute the importance score of each feature variable and consequently access the relative importance for all feature variables (e.g., EMG channels).

More precisely random forests use for the construction of each tree, a different bootstrap sample set from the original data. One-third of the samples are left out of the bootstrap sample set (out-of-bag samples) and are not used in the construction of the N th tree. Feature variables importance, is computed as follows; in every grown tree in the forest, we put down the out-of-bag samples and count the number of votes cast for the correct class. Then the values of a variable m are randomly permuted in the out-of-bag samples and these samples are put down the tree. Subtracting the number of votes casted for the correct class in the m -variable permuted out-of-bag data from the previously computed number of votes for the correct class in the untouched out-of-bag data, we get the importance score of a feature variable m for each tree. The raw importance score for each feature variable m is the average importance score for all trees of the random forest. The random forests feature variable importance calculation procedure, is depicted in Fig. 1.17.

In case that we want to reduce the number of EMG channels used (in this study we have already used 15 and 16 EMG channels), random forests can be initially run with all the variables (EMG channels) and then run once again with the most important variables selected during the first run. For example, we can use the

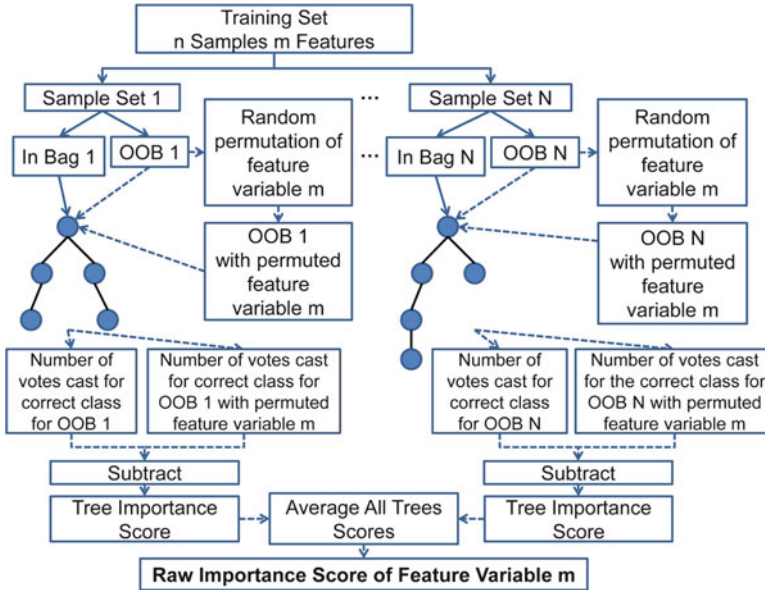


Fig. 1.17 Diagram of the random forests feature variable importance calculation procedure. OOB stands for out-of-bag samples

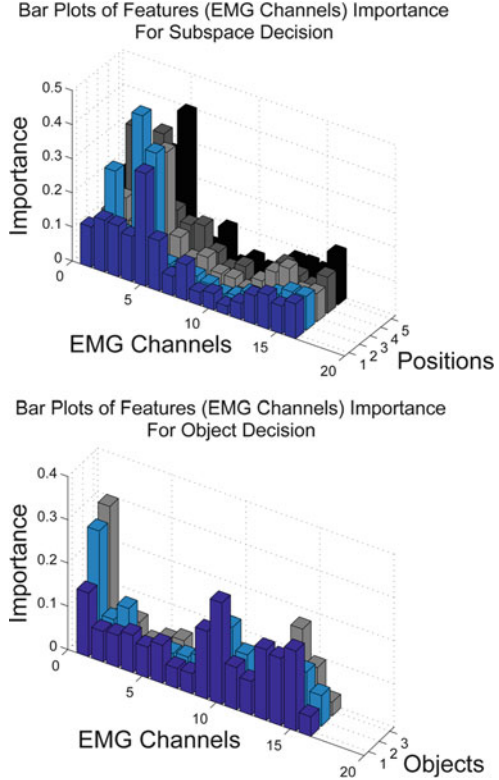
random forests classifier with all 15 EMG channels, compute the feature variables importance and re-solve the classification problem, using the most “important” EMG channels. Before doing so, we present the feature variables importance for the problems of discriminating from EMG signals, reach to grasp movements towards, different subspaces, different objects and different tasks.

In Fig. 1.18 we present the importance plots of different feature variables (EMG channels), for two different cases, subspace discrimination and object discrimination. We can notice that for subspace discrimination, the feature variables corresponding to upper-arm muscles (first 8 EMG channels) appear to have increased importance, while for object discrimination the feature variables corresponding to the forearm muscles (last 8 EMG channels), accumulate most of the importance.

This latter evidence can also be verified by the fact that for reach to grasp movements towards different subspaces, the muscular co-activation patterns of the upper-arm muscles accumulate most of the differentiation, while for reach to grasp movements towards different objects, the muscular co-activation patterns of the forearm muscles (responsible for grasping), accumulate most of the differentiation. More details can be found in [34].

In Fig. 1.19 we present the importance plots for different feature variables (EMG channels), for task discrimination. Four different barplots are depicted, that contain the importance scores per variable for different objects placed in position I. We can notice that the feature variables corresponding to the forearm muscles (last 8 EMG channels) appear to have once again increased importance

Fig. 1.18 Importance plots of feature variables (EMG channels) – expressed as mean decrease in accuracy – for Subject I, for subspace and object discrimination respectively. For subspace discrimination data involving all objects are used, while for object discrimination, a specific position is used (Pos I). Positions 1–5 correspond to positions Pos I to Pos V. Objects 1, 2 and 3 correspond to mug, marker and rectangle respectively



(similarly to object discrimination), since the forearm muscles are responsible for hand preshaping, in order to grasp and/or manipulate objects.

1.4.1 Task Specific Motion Decoding Models

1.4.1.1 Task Specific EMG Based Motion Decoding Models Based on Random Forests Regression

The Random Forests technique can also be used for regression, growing trees depending on a random vector Θ such that the tree predictor $h(\mathbf{x}, \Theta)$ takes on numerical values (not class labels used for classification). The random forest predictor, is formed similarly to the classification case, as appeared in Fig. 1.16, by taking instead of the most popular class, the average over the N trees of the forest $\{h(\mathbf{x}, \Theta_N)\}$.

Some advantages of the random forests regression are the following:

- Are easily implemented and trained.
- Are very fast in terms of time spent for training and prediction.

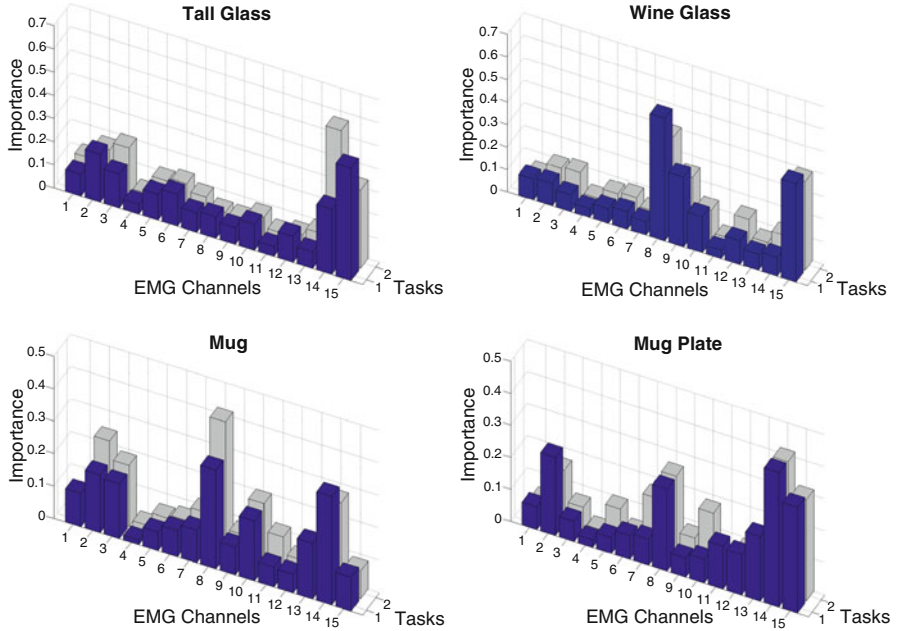


Fig. 1.19 Importance plots of feature variables (EMG channels) for task discrimination. Reach to grasp movements towards all objects placed in Position I were performed, so as to execute two different tasks per object. A list of the tasks executed can be found in Fig. 1.2

- Can be parallelized.
- Can handle thousands of input variables and run efficiently on large databases (similarly to classification).
- Are resistant to outliers.
- Have very good generalization properties.
- Can output more information than just class labels (e.g., sample proximities, visualization of output decision trees etc.).

1.4.1.2 Dimensionality Reduction

In order to formulate the regression problem used in this study, we need the low-dimensional spaces of the myoelectric activations and the human motion. Thus, in order to represent our data in low-d spaces, we used the Principal Components Analysis (PCA), dimensionality reduction method. For the EMG signals recorded, a 4-D space suffices, representing most of the original high-dimensional data variance (more than 92 %). Regarding the human arm hand system kinematics, a 4-D space once again suffices to describe adequately the 27-DoF motion of the human arm hand system, representing most (94 %) of the original data variance. We chose to

use the PCA as a dimensionality reduction technique – in order to take advantage of the underlying covariance of our data – representing also the same variability in a low-d space, without losing important information of the original data. More details regarding the employment of PCA in EMG based interfaces, can be found in [2].

1.5 Results

1.5.1 Classifiers Comparison

In order to validate our hypothesis that random forests based classification is an ideal method for EMG based interfaces, we have applied a wide variety of classification techniques in our dataset, comparing them with random forests, in terms of classification accuracy and time required for training.

More precisely, we performed Support Vector Machines (SVM) based classification (with a Radial Basis Function (RBF) kernel), we constructed a single hidden-layer Neural Network (NN) with ten hidden units (trained with the Levenberg-Marquardt backpropagation algorithm) and we used the k nearest neighbors (kNN) classifier, for the simplest case where $k = 3$. Finally random forests were grown with ten trees for speed. Random Forests outperformed the classification performance of all other classifiers and performed quite well in terms of speed of execution. More details regarding the comparison of classification results, can be found in [34].

The classification success rate (classification accuracy) is defined, as the percentage of EMG data points classified to the correct reach to grasp movement. It must be noted that the classification is done for every acquired EMG data point, thus the proposed learning scheme is able to decide in real-time the reach to grasp movement to be performed (for a specific task), and even switch to different tasks online. All classification results presented in this section, are the average values over the five rounds, of the five-fold cross-validation method applied.

The training dataset that was used to compare classifiers in terms of speed of execution, involved Subject 1 data of reach to grasp movements towards different objects, placed at Position I (Class I) and Position II (Class II). Results are reported in Table 1.1. All benchmarks were performed using MATLAB (Mathworks) in a standard PC with Intel(R) Core(TM) I5 CPU 611 @3.33 GHz and 4 GB RAM (DDR3) memory.

The training dataset that was used to compare classifiers in terms of classification accuracy, involved Subject 1 data of reach to grasp movements towards two objects (two classes), placed across three different positions in 3D space. Results are reported in Table 1.2.

Table 1.1 Comparison of classifiers in terms of time required for training

Classifiers	Samples	Training time (s)
LDA	2 classes of 1,500	0.011
	2 classes of 15,000	0.058
QDA	2 classes of 1,500	0.005
	2 classes of 15,000	0.051
kNN	2 classes of 1,500	0.014
	2 classes of 15,000	1.65
ANN	2 classes of 1,500	1.06
	2 classes of 15,000	16.05
SVM	2 classes of 1,500	0.34
	2 classes of 15,000	7.09
Random forests	2 classes of 1,500	0.06
	2 classes of 15,000	0.87

Table 1.2 Comparison of classifiers for discriminating two different reach to grasp movements, towards two objects placed across three different positions in 3D space, for Subject 1

Classifiers	Positions	Mug (%)	Rectangle (%)
LDA	Pos I	96.75	83.36
	Pos III	96.50	90.40
	Pos V	91.44	95.00
QDA	Pos I	95.34	80.52
	Pos III	97.30	91.45
	Pos V	92.30	95.60
kNN	Pos I	96.33	81.63
	Pos III	98.20	94.50
	Pos V	96.50	98.68
ANN	Pos I	94.67	84.63
	Pos III	98.50	94.76
	Pos V	94.52	98.87
SVM	Pos I	97.46	87.42
	Pos III	98.81	94.50
	Pos V	98.00	96.50
Random forests	Pos I	99.67	89.02
	Pos III	100	96.50
	Pos V	98.87	99.00

1.5.2 Comparison of Different Decoding Methods

In order to validate our hypothesis that random forests based regression is an ideal method for EMG based interfaces, we have applied also a wide variety of regression techniques in our data, comparing them with random forests, in terms of estimation accuracy and time spent for training. More specifically we performed Multiple Linear Regression (MLR), we created a State-Space model as described in [2], we performed SVM regression (with a RBF kernel) and we constructed a single hidden layer Neural Network with ten hidden units (trained with the Levenberg-Marquardt backpropagation algorithm). Finally random forests were used as a regression technique, growing ten (10) decision trees, to increase speed of execution and computational efficiency.

Table 1.3 Time spend for the training procedure across different methods for a specific dataset (10,000 samples) that serves as a benchmark (average values)

Method	Time (s)
MLR	0.0054
State space	8.65
ANN	28.83
SVM	27.72
Random forests	5.89

Table 1.4 Comparison of different methods and estimation results, for specific position (Pos III) and specific object (Marker), for Subject 1. Average values for different validation set splittings

Method	Arm joints similarity (%)	Hand joints similarity (%)
MLR	81.60	84.31
State space	82.74	85.10
ANN	85.10	86.92
SVM	86.01	88.90
Random forests	86.93	90.42

The formulated regression problem, was to map the low-d space (4 dimensions) of the myoelectric activity (EMG signals), to the low-d space (4 dimensions) of the human motion. The low-d spaces of human myoelectric activations and human motion were extracted using the PCA method. Then the estimated low-d human motion was back-projected to the high-d space providing an estimate of the full human arm hand system kinematics (27 DoFs). As far as the estimation accuracy is concerned, we compared the methods for different datasets, estimating human motion for reach to grasp movements, towards different positions, as well as different objects placed at the same position.

Regarding training time, we chose to compare the different techniques in terms of time required for training, applying the various methods to a separate dataset, that serves as a benchmark. In Table 1.3, we can notice that random forests outperform most other techniques, in terms of speed of execution.

In Table 1.4 we can notice that random forests outperform also the other regression techniques, such as the Support Vector Machines (SVM) and the Artificial Neural Networks (ANN), in terms of estimation accuracy. In order to compare the different regressors a standard PC with an Intel(R) Core(TM) I5 CPU 611 @3.33 GHz, equipped with a 4 GB RAM (DDR3) memory, was once again used. The benchmark was performed using MATLAB (Mathworks). More information regarding the regression techniques comparison results, can be found in [35].

1.5.3 Classification Results

In Table 1.5, we present the classification results across different reach to grasp movements, for a specific position and three different objects (three classes) for all subjects, using the random forest method.

Table 1.5 Classification accuracy across different reach to grasp movements towards a specific position and three different objects (three classes), for all subjects (using random forests)

Positions	Objects (Classes)		
	Mug (%)	Marker (%)	Rectangle (%)
Pos I	87.82 (± 4.52)	91.15 (± 5.31)	88.82 (± 4.63)
Pos II	84.24 (± 5.99)	90.40 (± 4.52)	91.81 (± 5.41)
Pos III	84.78 (± 5.78)	86.72 (± 5.16)	85.39 (± 4.95)
Pos IV	83.24 (± 6.14)	84.17 (± 6.21)	86.93 (± 4.83)
Pos V	86.55 (± 4.39)	89.32 (± 3.81)	90.74 (± 3.78)

Table 1.6 Classification accuracy across different reach to grasp movements, for a specific object and five different object positions (five classes), for all subjects (using random forests)

Positions (Classes)	Objects		
	Mug (%)	Marker (%)	Rectangle (%)
Pos I	86.01 (± 4.16)	89.83 (± 4.01)	87.01 (± 6.57)
Pos II	83.76 (± 6.24)	87.95 (± 4.78)	88.43 (± 5.51)
Pos III	89.74 (± 3.41)	87.23 (± 4.92)	90.30 (± 4.01)
Pos IV	91.23 (± 2.39)	90.05 (± 4.86)	90.51 (± 3.92)
Pos V	91.80 (± 3.45)	92.34 (± 2.69)	90.90 (± 3.01)

Table 1.7 Classification accuracy across different reach to grasp movements towards different positions, for all objects and subjects (using random forests)

Positions				
Pos I (%)	Pos II (%)	Pos III (%)	Pos IV (%)	Pos V (%)
88.51	86.29	87.91	89.20	91.02

In Table 1.6 we present the classification accuracy across different reach to grasp movements, for a specific object and five different object positions (five classes), for all subjects, using the random forest method.

In Table 1.7 we present the classification accuracy of random forest models, across reach to grasp movements towards five different positions (five classes), for all objects and subjects, using the random forest method.

In Table 1.8, we present the classification results achieved, using 15 EMG channels to discriminate between reach to grasp movements, towards specific position and object combinations (for all objects and positions), to execute two different tasks per object (two classes). As it can be noticed, classification accuracy is consistently high across different positions, different objects and different tasks. The latter evidence proves the efficiency of the proposed scheme for various reach to grasp movements and tasks.

In Table 1.8, we reported some interesting classification results for task discrimination, using a lot of EMG channels (15 EMG channels) which typically may not be available, due to hardware, cost or other limitations. Thus in this work we use the random forests technique to compute the feature variables (EMG channels)

Table 1.8 Classification accuracy across different reach to grasp movements, towards different positions and objects, to execute two different tasks (two classes). Random forests classifier was used for 15 EMG channels, of Subject 1 data

Tall glass		
Tasks	Side grasp (%)	Front grasp (%)
Pos I	76.31 (± 7.41)	78.87 (± 4.72)
Pos II	89.77 (± 5.43)	87.88 (± 9.42)
Pos III	84.86 (± 8.27)	85.75 (± 2.38)
Pos IV	89.69 (± 5.61)	86.82 (± 8.06)
Pos V	87.56 (± 8.20)	90.36 (± 4.77)
Wine glass		
Tasks	Side grasp (%)	Stem grasp (%)
Pos I	84.14 (± 4.15)	85.20 (± 4.59)
Pos II	71.23 (± 5.19)	79.72 (± 9.31)
Pos III	66.64 (± 8.15)	77.71 (± 11.47)
Pos IV	87.98 (± 5.21)	89.02 (± 5.81)
Pos V	66.44 (± 8.66)	64.28 (± 7.62)
Mug		
Tasks	Handle grasp (%)	Top grasp (%)
Pos I	89.33 (± 6.66)	90.74 (± 6.78)
Pos II	79.77 (± 6.74)	82.31 (± 7.02)
Pos III	75.98 (± 9.63)	83.52 (± 7.03)
Pos IV	84.91 (± 3.83)	86.99 (± 5.20)
Pos V	77.83 (± 5.79)	77.36 (± 3.95)
Mug plate		
Tasks	Side-pinch grasp (%)	Top grasp (%)
Pos I	84.98 (± 2.52)	81.76 (± 4.99)
Pos II	89.58 (± 6.11)	92.76 (± 4.27)
Pos III	86.73 (± 7.57)	95.58 (± 1.92)
Pos IV	87.16 (± 6.59)	85.64 (± 9.86)
Pos V	91.62 (± 3.08)	90.78 (± 2.98)

importance for each position and object combination and resolve the classification problems for task discrimination, using the six most important EMG channels.

Results for task discrimination, using the most important EMG channels, are reported in Table 1.9. We can notice that even for the reduced number of feature variables (EMG channels), classification accuracy remains consistently high and the results are equal or better than the initial results (with the 15 EMG channels).

In the aforementioned results, is evident that the classification accuracy and the overall ability of our scheme to discriminate different reach to grasp movements, towards different tasks (executed with the same object), depends on:

- The “distance” (in the configuration space) between the final postures of the full human arm hand system, that correspond to different tasks.

For example the two tasks of the tall glass, mug and mug plate result to completely different human wrist angles (wrist motion strongly affects forearm muscles). Thus, for these tasks better classification results can be achieved, in contrast to the wine

Table 1.9 Classification accuracy across different reach to grasp movements, towards different positions and objects, to execute two different tasks (two classes), for Subject 1. Random forests were used with the six most important EMG channels selected using the features selection method

Tall glass		
Tasks	Side grasp (%)	Front grasp (%)
Pos I	81.43 (± 2.64)	79.91 (± 7.69)
Pos II	89.79 (± 7.35)	90.79 (± 7.97)
Pos III	82.84 (± 9.12)	88.76 (± 3.34)
Pos IV	89.82 (± 5.89)	87.71 (± 7.97)
Pos V	84.66 (± 9.98)	92.85 (± 4.14)
Wine glass		
Tasks	Side grasp (%)	Stem grasp (%)
Pos I	86.77 (± 3.72)	84.30 (± 3.77)
Pos II	74.50 (± 9.81)	81.20 (± 9.64)
Pos III	72.62 (± 8.66)	79.39 (± 13.56)
Pos IV	86.90 (± 8.40)	87.61 (± 5.95)
Pos V	63.41 (± 6.88)	64.24 (± 9.72)
Mug		
Tasks	Handle grasp (%)	Top grasp (%)
Pos I	87.17 (± 4.67)	87.85 (± 4.59)
Pos II	80.10 (± 7.36)	83.72 (± 5.87)
Pos III	77.90 (± 5.40)	81.43 (± 6.98)
Pos IV	85.35 (± 4.14)	84.98 (± 6.07)
Pos V	81.06 (± 8.29)	78.95 (± 9.57)
Mug plate		
Tasks	Side-pinch grasp (%)	Top grasp (%)
Pos I	84.34 (± 5.57)	83.60 (± 3.44)
Pos II	90.74 (± 4.59)	94.01 (± 3.49)
Pos III	85.55 (± 12.07)	95.61 (± 2.89)
Pos IV	86.74 (± 10.18)	83.79 (± 7.27)
Pos V	91.00 (± 2.23)	92.28 (± 3.03)

glass tasks that involve mainly finger motions and variations of the aperture (less differentiation of muscular co-activation patterns).

- The position of the object to be grasped, as different positions result to different classification accuracies for the same object and tasks.

For example for positions I and IV the classifier achieves better classification accuracy for wine glass and mug, while positions II and V achieves better results for tall glass and mug plate.

1.5.3.1 Majority Vote Criterion

Given the fact that the classification decision in our scheme is taken at a frequency of 1 kHz, we can use a sliding window of width N , in order for all the N samples to be used for the classification decision. Inside this window, we can use the Majority

Table 1.10 Classification accuracy across different reach to grasp movements of Subject 1, towards a specific object (Marker) and varying object position, using random forests and random forests with MVC (in a sliding window of $N = 50$ samples)

Object rectangle	Subject1				
	Pos I (%)	Pos II (%)	Pos III (%)	Pos IV (%)	Pos V (%)
Random forests	87.03	91.61	90.51	86.25	92.61
RF with MVC	100	100	100	100	100

Table 1.11 Estimation results for a specific object (a marker) across all five object positions, for Subject 1, using a random forests model

Position	Arm	Hand
	similarity (%)	similarity (%)
Pos I	83.78 \pm 4.01	83.43 \pm 13.77
Pos II	88.80 \pm 3.98	86.60 \pm 15.02
Pos III	86.93 \pm 3.95	90.42 \pm 10.47
Pos IV	89.47 \pm 6.25	83.73 \pm 16.12
Pos V	91.53 \pm 6.57	89.04 \pm 10.09
All	80.19 \pm 7.32	81.15 \pm 16.24

Vote Criterion (MVC), which classifies all the samples of a set of N samples, in the class that was the most common between them (the class gathering the most votes). The use of the majority vote criterion, can improve the classification results acquired with the proposed methods.

More details regarding the sliding window and the MVC can be found in [34] and [46]. In Table 1.10, we present improved classification results using the majority vote criterion in a sliding window of $N = 50$ samples, for Subject 1 performing reach to grasp movements, towards a specific object (marker) and varying object position.

1.5.4 Task Specific Motion Decoding Results

In this section we present the EMG-based motion estimation results, for reach to grasp movements towards three different objects, placed at five different positions in 3D space. Highly accurate estimation results are achieved using task-specific random forest models, triggered from our scheme, taking into account the classification decision on the “task” to be executed.

More specifically in Table 1.11 we present estimation results for five subspace specific models, trained with Subject 1 data, to decode human motion during reach to grasp movements, towards five different positions to grasp a specific object (marker). In Table 1.12 we present estimation results for three object specific models, trained with Subject 1 data, to decode human motion during reach to grasp movements, towards a specific position (Pos I), to grasp three different objects (a marker, a rectangle and a mug).

Table 1.12 Estimation results for a specific position (Pos III) and all three different objects, for Subject 1, using a random forests model

Object	Arm similarity (%)	Hand similarity (%)
Marker	86.93 \pm 3.95	90.42 \pm 10.47
Rectangle	87.76 \pm 4.13	82.33 \pm 12.31
Mug	89.62 \pm 5.13	83.52 \pm 13.57
All	83.26 \pm 7.2	80.47 \pm 11.72

Table 1.13 Estimation results for specific position (Pos III) and specific object (a rectangle), for all subjects using a random forests model

Subject	Arm similarity (%)	Hand similarity (%)
Subject 1	87.76 \pm 4.13	82.33 \pm 10.47
Subject 2	85.91 \pm 6.21	81.59 \pm 11.78
Subject 3	89.44 \pm 4.30	84.93 \pm 14.93
Subject 4	87.32 \pm 5.34	85.28 \pm 10.16
Subject 5	82.11 \pm 7.79	80.54 \pm 16.32

In Tables 1.11 and 1.12 we can notice, that the models trained for each position or object separately, outperformed the “general” models built for all positions (for a marker) and all objects (placed at specific position, Pos III). With the term “general” models we mean those models trained for all positions in 3D space or all objects placed at a specific position (training of “general” models requires a training set that contains data for all classes of a specific problem).

Finally in Table 1.13 its evident, that the estimation results were usually better for the human arm (better estimation accuracy for human arm motion was achieved) than for the case of the human hand (human fingers motion). Such a finding, supports the applicability of our method, since precisely estimating the position of the human arm hand system end-effector (wrist), is far more important than fingers placement.

Similarity between the estimated and the captured human motion is defined as:

$$S = 100(1 - RMS(q_c - q_e)/RMS(q_c))\% \quad (1.1)$$

where RMS is:

$$RMS(q_c - q_e) = \sqrt{\frac{\sum_{i=1}^n (q_c - q_e)^2}{n}} \quad (1.2)$$

where q_c are the captured joint values, q_e the estimated joint values and n the number of samples. In Fig. 1.20 we compare the estimated from the task-specific model, user’s wrist position, with the user’s wrist position captured using the Isotrak II motion capture system, during the experiments. The data used are part of a validation set, not previously seen during training.

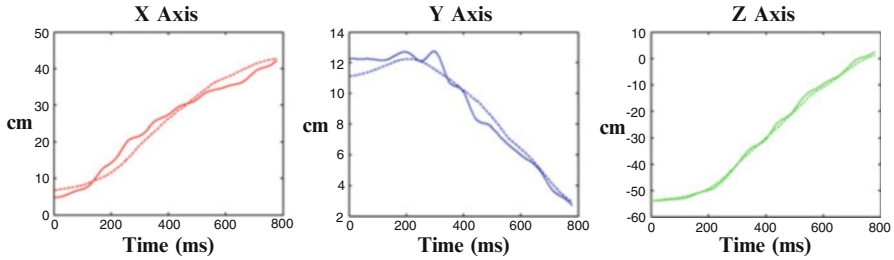


Fig. 1.20 EMG-based human end-effector (wrist) position estimation (using a task-specific motion decoding model). *Straight lines* represent the captured values (during the experiments), while the *dashed lines* represent the estimated values

1.6 Conclusions

A complete learning scheme for EMG based interfaces, has been proposed. A regressor and a classifier cooperate advantageously in order to split the task space, and achieve better motion decoding for reach to grasp movements, using task specific models. Thus, the proposed scheme is formulated so as to first discriminate between different reach to grasp movements, providing an appropriate classification decision and then trigger a task-specific EMG based motion decoding model, that achieves better motion estimation, than the “general” models. Principal Component Analysis (PCA) is used to represent in low dimensional manifolds the human myoelectric activity and the human motion. The regression problem is then formulated using these low-dimensional embeddings. The estimated output (human motion) can be back projected in the high dimensional space (27 DoFs), in order to provide an accurate estimate of the full human arm-hand system motion. The proposed scheme can be used by a series of EMG-based interfaces and for applications that range from human computer interaction and human robot interaction, to rehabilitation robotics and prosthetics. Regarding future research directions, we plan to apply the proposed scheme for the EMG based teleoperation of the robot arm-hand system Mitsubishi PA10 DLR/HIT II, taking into account the non-stationary characteristics of the EMG signals.

References

1. Graupe D, Salahi J, Kohn KH (1982) Multifunctional prosthesis and orthosis control via microcomputer identification of temporal pattern differences in single-site myoelectric signals. *J Biomed Eng* 4(1):17–22
2. Artemiadis PK, Kyriakopoulos KJ (2010) EMG-based control of a robot arm using low-dimensional embeddings. *IEEE Trans Robot* 26(2):393–398
3. Vogel J, Castellini C, van der Smagt PP (2011) EMG-based teleoperation and manipulation with the DLR LWR-III. In: *IEEE/RSJ international conference on intelligent robots and systems (IROS)*, San Francisco, pp 672–678

4. Cipriani C, Zaccone F, Micera S, Carrozza MC (2008) On the shared control of an EMG-controlled prosthetic hand: analysis of user prosthesis interaction. *IEEE Trans Robot* 24(1):170–184
5. Lucas L, DiCicco M, Matsuoka Y (2004) An EMG-controlled hand exoskeleton for natural pinching. *J Robot Mech* 16(5):482–488
6. Costanza E, Inverso SA, Allen R, Maes P (2007) Intimate interfaces in action: assessing the usability and subtlety of EMG-based motionless gestures. In: *Proceedings of the SIGCHI conference on human factors in computing systems, ser. CHI '07, San Jose. ACM, New York*, pp 819–828
7. Saponas TS, Tan DS, Morris D, Balakrishnan R (2008) Demonstrating the feasibility of using forearm electromyography for muscle-computer interfaces. In: *Proceedings of the twenty-sixth annual SIGCHI conference on human factors in computing systems, ser. CHI '08, Florence. ACM, New York*, pp 515–524
8. Thakur PH, Bastian AJ, Hsiao SS (2008) Multidigit movement synergies of the human hand in an unconstrained haptic exploration task. *J Neurosci* 28(6):1271–1281
9. Santello M, Flanders M, Soechting JF (1998) Postural hand synergies for tool use. *J Neurosci* 18(23):10105–10115
10. Todorov E, Ghahramani Z (2004) Analysis of the synergies underlying complex hand manipulation. In: *Proceedings of the 26th annual international conference of the IEEE engineering in medicine and biology society, EMBS '04, San Francisco, Sept 2004, vol 2*, pp 4637–4640
11. Mason CR, Gomez JE, Ebner TJ (2001) Hand synergies during reach-to-grasp. *AIP J Neurophys* 86(6):2896–2910
12. Klein Breteler MD, Simura KJ, Flanders M (2007) Timing of muscle activation in a hand movement sequence. *Oxf J Cereb Cortex* 17:803–815
13. Ajiboye AB, Weir RF (2009) Muscle synergies as a predictive framework for the EMG patterns of new hand postures. *J Neural Eng* 6(3):036004
14. Zajac FE (1986) Muscle and tendon: properties, models, scaling and application to biomechanics and motor control. In: *Bourne JR (ed) CRC critical reviews in biomedical engineering, vol 19, no 2. CRC, Boca Raton*, pp 210–222
15. Fukuda O, Tsuji T, Kaneko M, Otsuka A (2003) A human-assisting manipulator teleoperated by EMG signals and arm motions. *IEEE Trans Robot Autom* 19(2):210–222
16. Maier S, van der Smagt P (2008) Surface EMG suffices to classify the motion of each finger independently. In: *Proceedings of the international conference on motion and vibration control (MOVIC), Munich*
17. Bitzer S, van der Smagt P (2006) Learning EMG control of a robotic hand: towards active prostheses. In: *Proceedings 2006 IEEE international conference on robotics and automation (ICRA), Orlando, May 2006*, pp 2819–2823
18. Zhao J, Xie Z, Jiang L, Cai H, Liu H, Hirzinger G (2005) Levenberg-marquardt based neural network control for a five-fingered prosthetic hand. In: *Proceedings of the 2005 IEEE international conference on robotics and automation, ICRA, Barcelona, Apr 2005*, pp 4482–4487
19. Zecca M, Micera S, Carrozza MC, Dario P (2002) Control of multifunctional prosthetic hands by processing the electromyographic signal. *Crit Rev Biomed Eng* 30(4–6):459–485
20. Nishikawa D, Yu W, Yokoi H, Kakazu Y (1999) EMG prosthetic hand controller using real-time learning method. In: *IEEE SMC '99 conference proceedings: 1999 IEEE international conference on systems, man, and cybernetics, Tokyo, vol 1*, pp 153–158
21. Takahashi K, Nakauke T, Hashimoto M (2007) Remarks on hands-free manipulation using bio-potential signals. In: *IEEE international conference on systems, man and cybernetics, Montreal, Oct 2007*, pp 2965–2970
22. Castellini C, Fiorilla AE, Sandini G (2009) Multi-subject/daily-life activity EMG-based control of mechanical hands. *J Neuroeng Rehabil* 6:1–11
23. Brochier T, Spinks RL, Umilta MA, Lemon RN (2004) Patterns of muscle activity underlying object-specific grasp by the macaque monkey. *J Neurophysiol* 92(3):1770–1782

24. Hill A (1938) The heat of shortening and the dynamic constants of muscle. *Proc R Soc Lond Ser B* 126(843):136–195
25. Cavallaro E, Rosen J, Perry J, Burns S, Hannaford B (2005) Hill-based model as a myoprocessor for a neural controlled powered exoskeleton arm – parameters optimization. In: *Proceedings of the 2005 IEEE international conference on robotics and automation, ICRA, Barcelona, Apr 2005*, pp 4525–4530
26. Artemiadis P, Kyriakopoulos K (2005) Teleoperation of a robot manipulator using EMG signals and a position tracker. In: *IEEE/RSJ international conference on intelligent robots and systems (IROS), Edmonton, Aug 2005*, pp 1003–1008
27. Potvin J, Norman R, McGill S (1996) Mechanically corrected EMG for the continuous estimation of erector spinae muscle loading during repetitive lifting. *Eur J Appl Physiol Occup Physiol* 74:119–132
28. Lloyd DG, Besier TF (2003) An emg-driven musculoskeletal model to estimate muscle forces and knee joint movements in vivo. *J Biomech* 36:765–776
29. Artemiadis P, Kyriakopoulos K (2011) A switching regime model for the EMG-based control of a robot arm. *IEEE Trans Syst Man Cybern B Cybern* 41(1):53–63
30. Artemiadis P, Kyriakopoulos K (2007) EMG-based teleoperation of a robot arm using low-dimensional representation. In: *IEEE/RSJ international conference on intelligent robots and systems, IROS 2007, San Diego, 29 Oct 2007–2 Nov 2007*, pp 489–495
31. Smith RJ, Tenore F, Huberdeau D, Etienne-Cummings R, Thakor NV (2008) Continuous decoding of finger position from surface EMG signals for the control of powered prostheses. In: *30th annual international conference of the IEEE engineering in medicine and biology society, EMBS, Vancouver, Aug 2008*, pp 197–200
32. Ryu W, Han B, Kim J (2008) Continuous position control of 1 dof manipulator using EMG signals. In: *Third international conference on convergence and hybrid information technology, ICCIT '08, Busan, vol 1, Nov 2008*, pp 870–874
33. Koike Y, Kawato M (1995) Estimation of dynamic joint torques and trajectory formation from surface electromyography signals using a neural network model. *Biol Cybern* 73:291–300
34. Liarokapis MV, Artemiadis PK, Katsiaris PT, Kyriakopoulos KJ, Manolakos ES (2012) Learning human reach-to-grasp strategies: towards EMG-based control of robotic arm-hand systems. In: *IEEE international conference on robotics and automation (ICRA), St. Paul, May 2012*, pp 2287–2292
35. Liarokapis MV, Artemiadis PK, Katsiaris PT, Kyriakopoulos KJ (2012) Learning task-specific models for reach to grasp movements: towards EMG-based teleoperation of robotic arm-hand systems. In: *4th IEEE RAS EMBS international conference on biomedical robotics and biomechanics (BioRob), Rome, June 2012*, pp 1287–1292
36. Liarokapis MV, Artemiadis PK, Kyriakopoulos KJ, Manolakos ES (2013) A learning scheme for reach to grasp movements: on EMG-based interfaces using task specific motion decoding models. *IEEE J Biomed Health Inform* 17(5):915–921
37. Fligge N, Urbanek H, van der Smagt P (2012) Relation between object properties and emg during reaching to grasp. *J Electromyogr Kinesiol* 23(2):402–410
38. Liarokapis MV, Artemiadis PK, Kyriakopoulos KJ (2013) Task discrimination from myoelectric activity: a learning scheme for EMG-based interfaces. In: *IEEE international conference on rehabilitation robotics (ICORR), Seattle, June 2013*, pp 1–6
39. Artemiadis PK, Katsiaris PT, Kyriakopoulos KJ (2010) A biomimetic approach to inverse kinematics for a redundant robot arm. *Auton Robots* 29(3–4):293–308
40. Liarokapis MV, Artemiadis PK, Kyriakopoulos KJ (2012) Functional anthropomorphism for human to robot motion mapping. In: *21st IEEE international symposium on robot and human interactive communication (RO-MAN), Paris, Sept 2012*, pp 31–36
41. Cram JR, Kasman GS, Holtz J (1998) *Introduction to surface electromyography*. Gaithersburg, Md., Aspen Publishers.
42. Dae Hyong K et al (2011) Epidermal electronics. *Science* 333:838–843
43. Sheskin DJ (2007) *Handbook of parametric and nonparametric statistical procedures*, 4th edn. Chapman & Hall/CRC, Boca Raton

44. Ho TK (1995) Random decision forests. In: Proceedings of the third international conference on document analysis and recognition, Montréal, Aug 1995, vol 1, pp 278–282
45. Breiman L (2001) Random forests. *Mach Learn* 45(1):5–32
46. Theodoridis S, Koutroumbas K (2009) *Pattern recognition*, 4th edn. Academic/Elsevier Science, Amsterdam/London